Canadian Mineralogist
Vol. 26, pp. 721-736 (1988)

EXPLORATION FOR HYDROTHERMAL ACTIVITY NEAR THE RODRIGUEZ TRIPLE JUNCTION, INDIAN OCEAN

PETER M. HERZIG* AND WALTER L. PLÜGER**

Institut für Mineralogie and Lagerstättenlehre, Rheinisch-Westfälische Technische Hochschule Aachen, D-5100 Aachen, Federal Republic of Germany

ABSTRACT

The Central Indian Ridge between 21°–24°S, near the Rodriguez Triple Junction, was investigated by RV *SONNE* during the 1983 and 1986 cruises of the GEMINO project (Geothermal Metallogenesis Indian Ocean) for the purpose of locating sites of hydrothermal activity. In response to reconnaissance data of conductive heat flow, sediment cores, and hydrocasts, two intermediate spreading ridge segments at 21.5°S (area EX/FX) and 23°S (area JX) were selected for detailed exploration including mapping, sampling and visual seafloor observation. Hydrothermally influenced sediment cores and altered basalts were found in both study areas. Total dissolvable Mn concentrations up to 27.5 nmol/kg and CH_4 values up to 45.6 nL/L occur within 450 m above bottom in the northern and southern overlapping propagators in area EX/FX. In addition, δ^3He values up to 18.6% and a potential temperature anomaly (0.01°C) were found. In area JX, maximum concentrations of 36.1 nL/L CH_4 and 10.7 nmol/kg total dissolvable Mn in the water column seem to be related to a central neovolcanic ridge close to a ridge-transform intersection. At the eastern flank of this ridge, a significant potential temperature anomaly of 0.04°C was measured. The results obtained in areas EX/FX and JX provide evidence for hydrothermal activity. However, in comparison to the TAG hydrothermal field at the Mid-Atlantic Ridge at 26°N, the data indicate a more restricted and probably lower temperature hydrothermal discharge.

Keywords: hydrothermal activity, exploration, Southern Central Indian Ridge, Rodriguez Triple Junction, bathymetry, sediments, basalts, methane, manganese, helium.

SOMMAIRE

Nous avons étudié la crête océanique médio-indienne entre 21° et 24°S, près du point triple de Rodriguez, au cours des expéditions de 1983 et 1986 du RV *SONNE*: notre étude, effectuée dans le cadre du projet GEMINO (Geothermal Metallogenesis Indian Ocean), avait pour but de trouver des sites d'activité hydrothermale. À la suite de données préliminaires sur le flux de chaleur par conduction, des carottes de sédiments, et des sites de relevés hydrographiques, nous avons choisi deux régions le long de l'axe de séparation des plaques, une à 21.5°S (EX/FX) et l'autre à 23°S (JX), afin d'effectuer un relevé cartographique, un échantillonnage et une observation visuelle plus approfondis du plancher sub-océanique. Les deux endroits se caractérisent par des carottes de sédiments montrant des phénomènes hydrothermaux et des basaltes altérés. La concentration totale de Mn soluble atteint 27.5 nmol/kg, et des concentrations de 45.6 nL/L de CH_4 sont décelées à 450 m au dessus du fond le long des systèmes de propagation septentrionaux et méridionaux dans la région de EX/FX. De plus, nous avons trouvé des valeurs de δ^3He pouvant atteindre 18.6%, et une anomalie géothermique possible de 0.01°C. Dans le domaine JX, les concentrations maximales de 36.1 nL/L de CH_4 et de 10.7 nmol/kg de Mn soluble dans la colonne d'eau semblent liées à la crête néovolcanique centrale, près d'une intersection de la crête et d'une faille transformante. Le long du flanc oriental de cette crête, nous avons décelé une anomalie géothermique potentielle importante de 0.04°C. Nos résultats témoignent d'une activité hydrothermale dans les deux endroits. Toutefois, comparées à l'activité dans le champ hydrothermal de TAG, à 26°N le long de la crête médio-atlantique, nos données indiquent une décharge hydrothermale plus restreinte et probablement de température plus basse.

(Traduit par la Rédaction)

Mots-clés: activité hydrothermale, exploration, crête océanique médio-indienne, point triple de Rodriguez, bathymétrie, sédiments, basaltes, méthane, manganèse, hélium.

INTRODUCTION

Although many active and inactive hydrothermal sites have been found at medium- to fast-spreading (5–18 cm/yr) oceanic ridges in the Pacific Ocean within the last 10 years (Corliss *et al.* 1979, Francheteau *et al.* 1979, Lonsdale *et al.* 1980, Spiess *et al.* 1980, Hékinian *et al.* 1981, Normark *et al.* 1982a,

** and GEMINO-1/-2 Shipboard Scientific Parties: K. Becker, G. Deissmann, A.P. O'Kelly, D. Schöps (Technische Hochschule Aachen); J. Scholten (Bundesanstalt für Geowissenschaften und Rohstoffe, Hannover); A. Yelles-Chaouche (Institut de Physique du Globe, Paris, France); T. Ashis Ghosh, V.N. Kodagali, R. Mukhopadhyay, B. Nagender Nath, T. Ramprasad, P. Sivasankara Rao (National Institute of Oceanography, Goa, India); F. Bayer, D. Hansen, J. Lange, O. Lettau, W. Pohl (Preussag, Hannover); H. Kunzendorf (Risø National Laboratory, Denmark); W. Michaelis, B. Mycke, R. Seifert (Universität Hamburg); P. Walter (Universität Heidelberg); P. Stoffers (Universität Kiel).

* Present address: Marine Geology Research Group, Department of Geology, University of Toronto, Toronto, Ontario M5S 1A1, Canada.

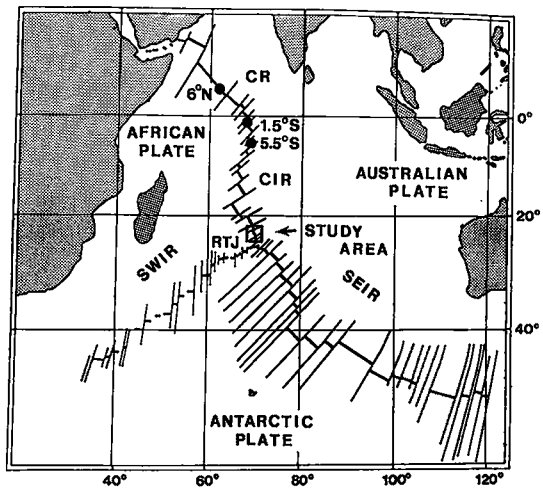

FIG. 1. Location of the GEMINO–2 study area (square), north of the Rodriguez Triple Junction (RTJ). The Carlsberg Ridge (CR) and Central Indian Ridge (CIR) at 6°N, 1.5°S and 5.5°S were investigated during GEMINO–1. SWIR and SEIR refer to the South West Indian and South East Indian Ridges, respectively.

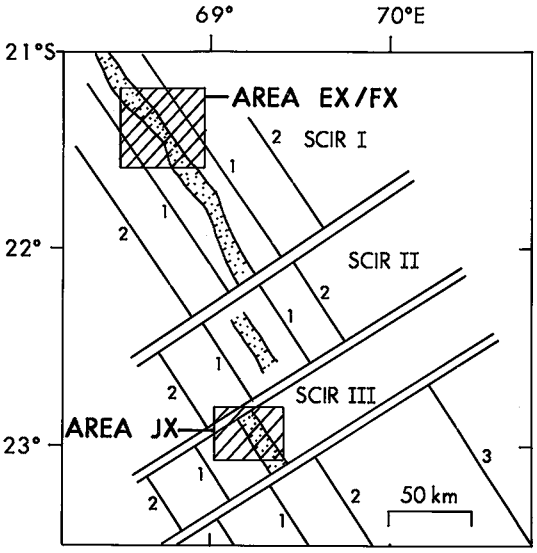

FIG. 2. Location of ridge segments I, II and III of the SCIR (Southern Central Indian Ridge) and target areas EX/FX and JX. Approximate outline of the rift valley indicated by stippling; double lines indicate transform faults. Also shown are magnetic anomalies 1 to 3, representing crust of 0.7, 1.9 and 4.7 Ma age, respectively (R. Schlich and our unpubl. data).

Koski *et al.* 1982, Scott *et al.* 1984), sulfide mineralization was unknown from the poorly investigated, low- to medium-rate spreading ridges in the Atlantic and the Indian Ocean until 1985. In that year, the spectacular discovery of black smokers, massive sulfides and vent biota in the TAG (Trans-Atlantic Geotraverse) area at the Mid-Atlantic Ridge, 26°N (Rona *et al.* 1986) proved that hydrothermal phenomena are not related to the spreading rate and are probably a common feature at oceanic ridges in general.

In 1983 the GEMINO project (Geothermal Metallogenesis Indian Ocean) was initiated as the first large-scale exploration program for polymetallic sulfide deposits in the Indian Ocean. A 42-day reconnaissance survey with the German research vessel RV *SONNE* along the Carlsberg (CR) and Central Indian Ridge (CIR) (Fig. 1) was the first part of the campaign, and was aimed to verify previously reported hydrothermal mineralization at 6°N, 1.5°S and 5.5°S (Fig. 1) (Bäcker 1975, Rona *et al.* 1981, Rozanova & Baturin 1971). However, no sulfide mineralization or hydrothermal activity was located. An area north of the Rodriguez Triple Junction (RTJ) between 21°S and 24°S (Fig. 1) instead was chosen for further investigation in response to results obtained from heat-flow measurements, sediment cores, and water geochemistry (Plüger *et al.* 1984, Plüger 1985). In 1986, GEMINO–2 carried out detailed bathymetric mapping and exploration, using Mn and CH_4 as tracers in the water column, sediment and basalt composition, and visual seafloor observation. Although hydrothermal sulfide mineralization has not yet been located, target areas have been more narrowly defined (Plüger & Herzig 1986). This paper reports and discusses data collected by the GEMINO–1 and –2 expeditions and outlines evidence for hydrothermal activity on the CIR at 21.5°S (area EX/FX) and 23°S (area JX) (Fig. 2).

GEOLOGICAL AND STRUCTURAL SETTING

The Rodriguez Triple Junction (RTJ), located at about 25°30′S and 70°E (Fig. 1), represents the convergence point of the Indian, African and Antartic plates. The three associated ridges are the Central Indian Ridge (CIR), the Southeast Indian Ridge (SEIR), and the Southwest Indian Ridge (SWIR).

Close to the triple junction, the CIR and the SEIR have bathymetric characteristics of typical mid-ocean ridge spreading centers, exhibiting well-defined median valleys (Price *et al.* 1986). According to Tapscott *et al.* (1980) and Schlich *et al.* (1986), the CIR near the triple junction has been spreading symmetrically at a nearly constant half-rate of 2.7 cm/yr over the last 4 Ma. The central valley, which is 3500–4000 m deep and 5 to 8 km wide, shallows to <3000 m between 15°S and 22°S (Price *et al.* 1986). The SEIR prolongs the CIR as a medium-rate spreading ridge (3.0 cm/yr half-rate) with a rift valley about 14 km wide (Schlich *et al.* 1986). By contrast, the SWIR is a slow-spreading ridge

(0.8 cm/yr), which approaches the CIR and SEIR as an elongate, triangular deep (4500 m) with the apex at the RTJ (Tapscott *et al.* 1980).

The RTJ has played a major role in controlling the structural evolution of the Indian Ocean since the late Cretaceous (Schlich 1982). Sclater *et al.* (1981) have shown that the SWIR developed as a consequence of the rapid eastward movement of the triple junction during Eocene to present time. Schlich *et al.* (1986) favor a non-stable ridge–ridge–ridge model for the development of the RTJ within the last 10 Ma. They show a 5 km offset between the CIR and SEIR, and suggest that the SWIR close to the RTJ may correspond to a stretched area without spreading. Montigny *et al.* (1985) and Michard *et al.* (1986) concluded on the basis of rock geochemical studies that a hot spot does not exist below the RTJ. Instead, individual magma chambers are presumed to lie beneath each ridge around the RTJ (Schlich *et al.* 1986).

Three ridge segments termed SCIR (Southern Central Indian Ridge) I, II and III were investigated in the present study; however, most detailed work was carried out in areas EX/FX of SCIR I and JX of SCIR III (Fig. 2). The lengths of the segments are 190 km (SCIR I), 55 km (SCIR II), and 40 km (SCIR III). Interpretation of Seabeam and magnetic data collected by *RV SONNE* and R. Schlich (pers. comm. 1986) suggested that the segments are offset by deep, linear fracture zones trending about N45°E, which have caused a left-lateral displacement of the ridge axis.

Methods

Bathymetric mapping was carried out using the Seabeam sonar system aboard the *RV SONNE*. The Ocean Floor Observation System (OFOS) was available for camera tows. In addition to a real-time black and white TV camera, the OFOS carries a 35-mm still camera, and a color-video system. TV-guided grabs and conventional chain-bag dredges were used for rock sampling. Sediment sampling was carried out with box and gravity corers. For heat-flow measurements, 5 outrigger thermistors were mounted on the gravity corer. The thermal conductivity was determined according to the method of von Herzen & Maxwell (1959).

Water sampling was done using wire-mounted Niskin Go-flow bottles (5 liter) or a rosette sampler consisting of 12 remote-controlled Niskin bottles in combination with a CTD probe. Samples were taken either at 10, 35, 60, 110, 210, 410 m above bottom or every 25 m up to 150 m above bottom, and at 200, 500, 1000 and 2000 m.

For navigation of the ship, the global positioning system (GPS) gave locations within an estimated precision of 75 ±25 m when sufficient satellite coverage was available, usually about 7 hours per day. Some studies were carried out using conventional Satnav navigation, with an estimated accuracy of ±200–400 m.

Analytical Techniques

Mineralogical and chemical characterization of sediment and rock samples was done onboard and in the shore-based laboratory by XRD (Philips/Siemens D 500) and XRF (Philips PW 1410/PW 1400) using standard methods. Glass analyses were done with an ARL-SEMQ electron microprobe.

Total dissolvable Mn was determined in seawater samples collected in pre-cleaned 50 ml polyethylene bottles using the method of Grobenski *et al.* (1984) after acidification to pH <2 with 65% ultrapure HNO_3. Analyses were done onboard by atomic absorption using a Zeeman-corrected Perkin–Elmer 3030 Z spectrometer with graphite furnace. Seawater standards NASS-1 and CASS-1 (National Research Council of Canada) were measured as reference.

Samples for CH_4 determinations were taken by drawing water into 500 ml gas-tight glass bottles. Dissolved CH_4 was analyzed onboard, using the method of Swinnerton & Linnenbom (1967), and a Carlo Erba gas chromatograph 4200 with flame ionization detector. Water samples for He isotope measurements were collected using standard procedures (*e.g.*, Jenkins *et al.* 1979). Samples were analyzed on-shore following the mass spectrometrical method described by Roether (1983) and are reported as δ^3He (%) = 100 $(R_{sample}/R_{air}-1)$ where $R = {}^3He/{}^4He$.

Results

Rift geometry and bottom topography

As a basis for exploration, the areas EX/FX and JX were mapped at a scale of 1:20,000 with 20-m contour intervals. However, the bathymetric data in this paper are presented at a scale of 1:100,000 using 100-m contours.

Area EX/FX. Figure 3a shows the bathymetry of the EX/FX area, SCIR I segment. In this area the ridge flanks are about 8 to 10 km apart and rise to 2700 m (west side) and 2400 m (east side) depth, respectively. The asymmetrical rift valley (Fig. 4a) decreases in depth from >3500 m in the northwest to about 3100 m in the southeast, where a small central high occurs instead of a graben at 21°31′S. Here, the axial valley as defined by the 3000 m contour in Figure 3b narrows to less than 5 km. The along-strike bathymetric variation suggests that the overall topographic high (bathymetric minimum) lies toward the southeast. Several volcanic cones more than 200 m high occur throughout the rift valley.

The most prominent structural feature in the area is the discontinuation of the Neovolcanic Zone at

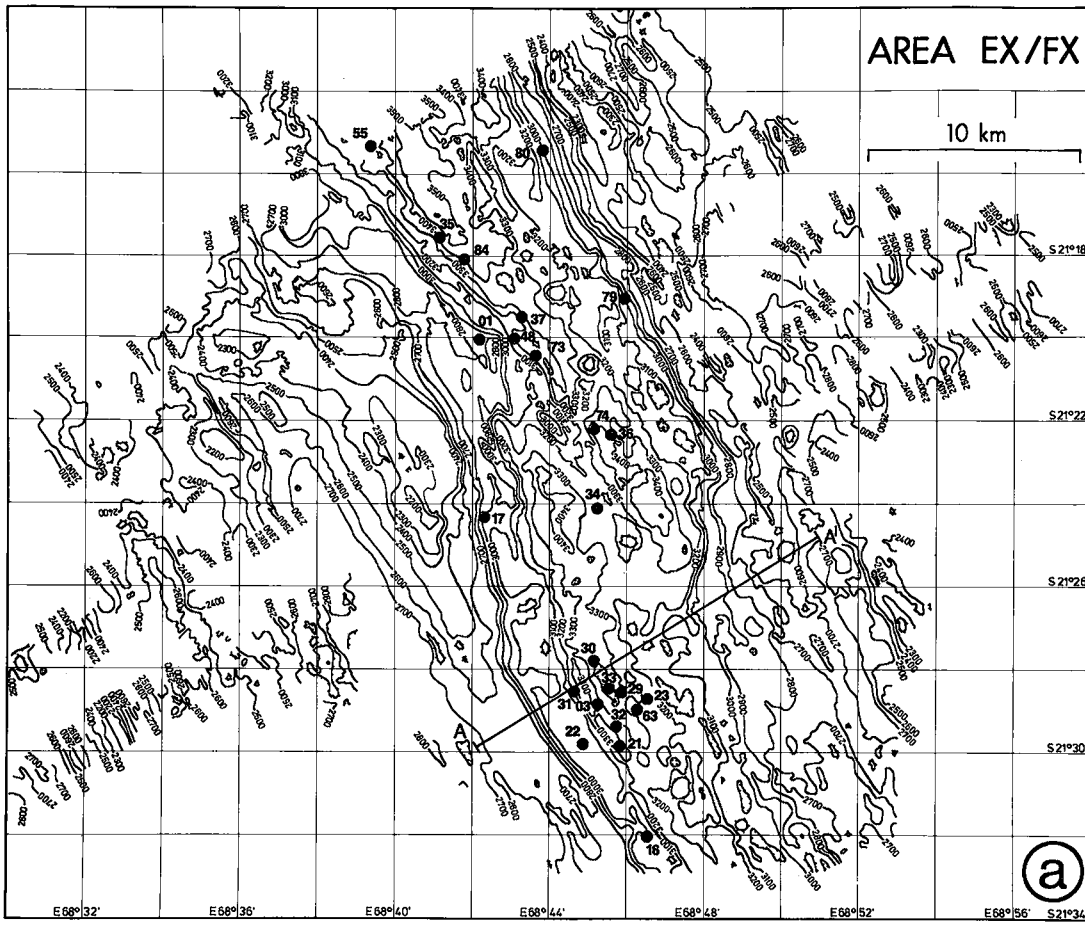

FIG. 3. (a) Seabeam bathymetry of study area EX/FX, covering a total of about 1100 km^2 (100-m contour intervals; uncorrected velocity 1500 m/s; GPS navigated). Line A–A′ refers to the line of section shown in Figure 4a. Locations of water-sampling stations are indicated by black dots.

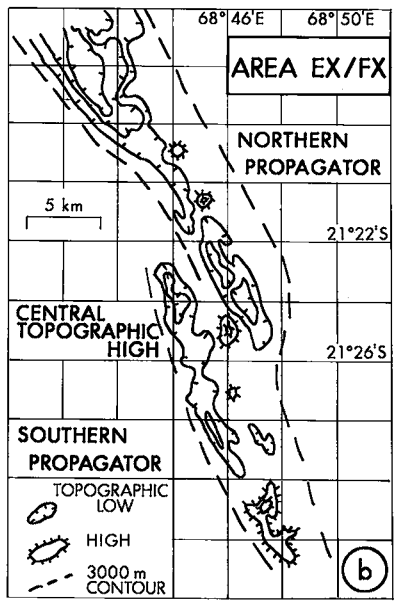

FIG. 3. (b) Schematic sketch of the same area as in (a), showing structural features referred to in text.

about 21°24′S (Fig. 3b). Here, the ridge axis is laterally offset about 4 km to the southwest, with an overlap of about 8 km. Thus, the two ridges constitute overlapping spreading centers. At fast-spreading ridges (*e.g.*, EPR), overlapping spreading centers appear to develop at small (<15 km) offsets instead of transform faults and are characterized by a central depression (Macdonald & Fox 1983). However, the overlapping spreading centers in area EX/FX enclose a 200 m topographic high.

Area JX. This area is bordered to the north by a fracture zone which reaches a depth of more than 3600 m in the northeast (Fig. 5a). The top of the western ridge flank decreases in depth along strike from 3200 m close to the fracture zone to less than 2600 m in the south. The eastern wall rises to about 2800 m and shows a series of steep slopes and small plateaus assumed to be created by normal faults. A distinctive central ridge more than 300 m high

extends about 15 km southeast from the fracture zone. The ridge divides the main valley into a wide and deep (>3800 m) western valley and a shallower, narrower, eastern valley (Figs. 4b, 5b). South of 22°59′S the ridge becomes a wide plateau at 3400 m depth. The axial valley (3000 m contour) narrows from 12 km in the north to about 8 km in the south (Fig. 5b). A small topographic high occurs at 23°03′S.

Sediment cover, lava types and tectonic features

Area EX/FX. OFOS seafloor observations reveal that volcanic rocks in the northern part of area EX/FX are overlain by 0–5 cm of sediment. The sediment cover decreases from 70–100% at the base of the eastern marginal high to <5% close to the axial graben. Within the axial graben, sediment accumulates only in basalt interstices. Pillow lavas with striations and protuberances are abundant adjacent to the rift valley, whereas fresh, glassy sheet flows, comprising lobate, scrambled and curtain-fold forms, predominate within the central neovolcanic zone. Small-scale fractures and fissures (0.1–1 m wide) are common. Dredge hauls recovered glassy sheet flows from the tip of the northern overlapping spreading center in the central EX/FX area. The topographic high enclosed within the overlap zone mainly consists of moderately sedimented sheet flows and pillows. This high probably represents pieces of old crust, trapped within the overlap zone. In the southern EX/FX area, pillow lavas predominate along the western ridge flank, and sheet flows with <5% sediment cover floor the axial graben. Fault scarps, with up to 40 m relief, and large talus piles occur at about 21°30′S. Volcanics of the southern central high at 21°31′S are fresh, glassy sheet flows.

Area JX. The central ridge that divides the main valley is made up of relatively fresh pillow lavas and sheet flows with little sediment cover, and is interpreted to be actively spreading. By contrast, the eastern and western valleys are heavily sedimented. The ridge flanks are fissured and fractured with openings centimeters to meters wide. Steep normal faults with meter-scale displacements are common. Moderately sedimented sheet flows predominate over pillow lavas on the axial plateau at 22°59′S. The topographic high at 23°03′S is characterized by glassy sheet flows varying among platy, curtain-fold, scrambled, lobate and nodular types. This sediment-dusted sheet-flow terrain has faults and fractures <1 m wide.

Basalt mineralogy and chemistry

To determine the degree of fractionation and the type of alteration, which are of interest for the exploration of hydrothermal mineralization (Thompson *et al.* 1985, Haymon & Kastner 1986), basalt samples were recovered from several locations in areas EX/FX and JX, including the axial graben, the valley floor, the eastern and western marginal highs, and small volcanic cones within the rift valley. Pillow fragments and pillow talus dominate the collection (>90%); sheet-flow fragments are less abundant (<10%). Fresh glass up to 1.0 cm thick occurs on pillow and sheet-flow surfaces from the central rift valley. Although most recovered basalts are generally porphyritic, those from the axial plateau in the southern area JX are aphyric, platy sheet-flow basalts.

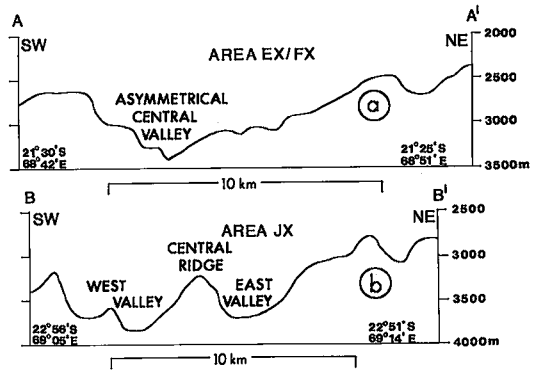

FIG. 4. Profiles perpendicular to the ridge axis in study areas EX/FX and JX. (a) Profile A–A′ illustrates the asymmetrical form of the narrow and V-shaped graben in the southern part of area EX/FX, south of the overlapping propagators. (b) Profile B–B′, in the northern part of area JX, shows a central ridge that divides the main valley into east and west valleys. Profile locations shown in Figure 3a and 5a.

Mineralogy. Plagioclase phenocrysts and microphenocrysts are abundant and occur in glassy margins as well as in crystalline interiors. Microprobe data show a compositional range of An_{72} to An_{83} and average An_{80}. Glass inclusions in plagioclase contain 8.50 wt.% MgO and 2.31% TiO_2 on average. The most albitic plagioclase occurs in a sheet-flow sample from the 3400-m plateau at 23°01′S in area JX (0.10% K_2O and 0.70% Fe_2O_3). Glass inclusions in plagioclase of this sample are more fractionated than in plagioclase from other locations.

Olivine (Fo_{84} to Fo_{88}, av. Fo_{86}) occurs within the crystalline upper and lower parts of sheet flows and in crystalline pillow margins. Glass inclusions chemically similar to those in plagioclase occur in the olivine. Pyroxene phenocrysts are present in only a few samples. Microscopic and XRD data indicate that pyroxene is diopsidic augite with a normative (CIPW) composition of $Wo_{50}En_{35}Fs_{15}$.

Using the nomenclature of Hékinian (1982), the samples recovered from areas EX/FX and JX can be classified as "moderately phyric plagioclase basalts". However, those from the southern area JX

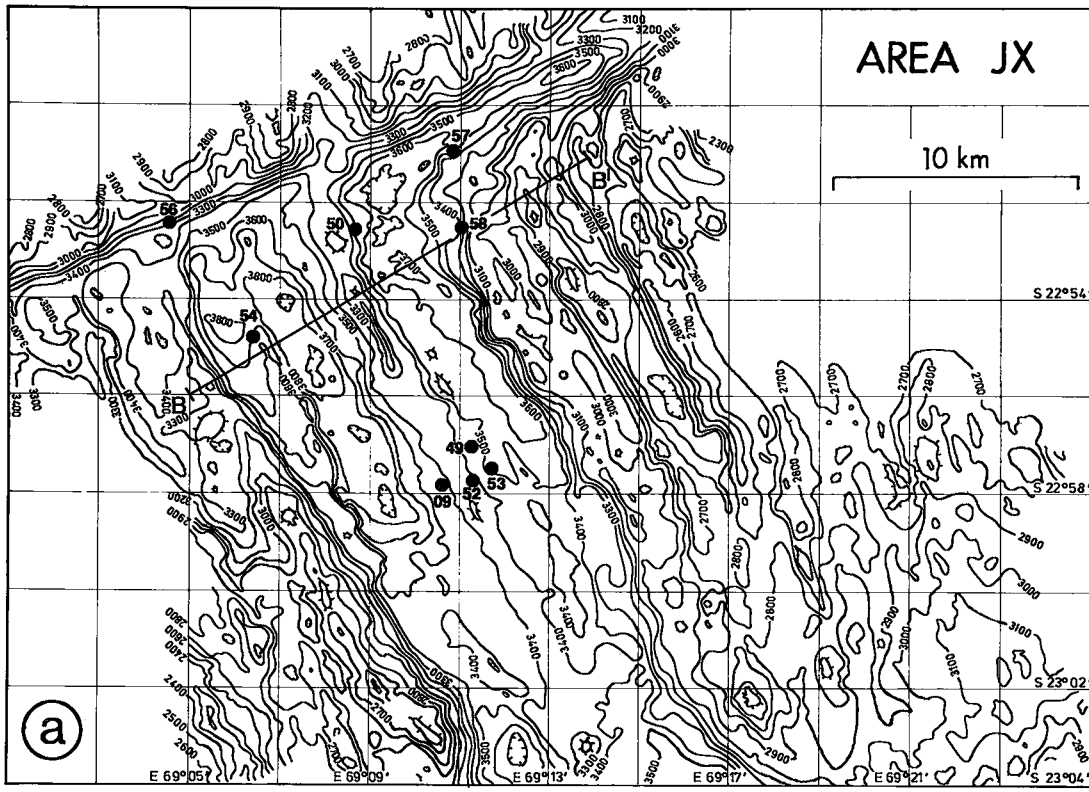

FIG. 5. (a) Seabeam bathymetry of study area JX, covering a total of about 900 km^2 (100 m contour intervals; uncorrected velocity 1500 m/s; GPS navigated). Line B–B′ refers to the line of section shown in Figure 4b. Locations of water sampling stations are indicated by black dots.

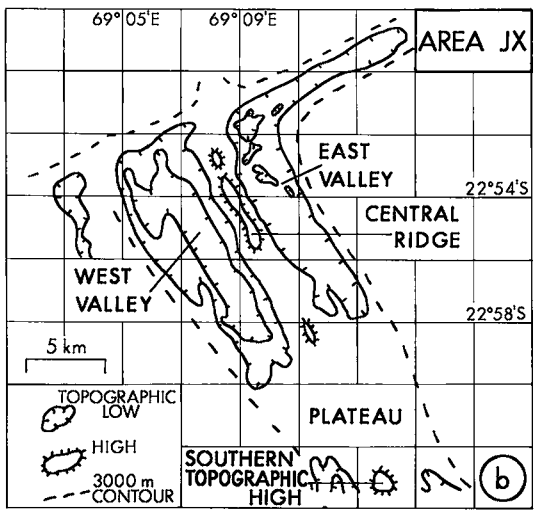

FIG. 5. (b) Schematic sketch of the same area as in (a), showing the structural features referred to in text.

(66 DR) are slightly more fractionated olivine tholeiites.

Whole-rock chemistry. The basalts contain 15.3–17.8 wt.% Al_2O_3 (Table 1), depending on the abundance of plagioclase phenocrysts. Most samples have 15.5–17.0% Al_2O_3, 1.1–1.4% TiO_2, and FeO_t/MgO ratios of 0.9–1.2; these values are typical of "moderately phyric plagioclase basalts" (Hékinian 1982). The average MgO content of 8.2% and the low alkali contents (Na_2O <2.5%, K_2O <0.15%) suggest that the majority of samples is primitive tholeiitic basalt, *i.e.*, depleted *N*-type MORBs. The Al-rich samples have low contents of TiO_2 (0.7–0.8%) and K_2O (0.06–0.10%), and FeO_t/MgO ratios of 0.8–1.0. All samples analyzed follow the same compositional trend in an FeO_t/MgO *versus* TiO_2 diagram (Fig. 6), and are considered to represent products of fractional crystallization. Sheet flows from the axial plateau in area JX are most fractionated. However, the variability of TiO_2 (0.7–1.5%) and K_2O (0.06–0.34%) at a given FeO_t/MgO ratio indicates that multiple parental magmas might be necessary to produce the range of lavas erupted.

TABLE 1. MAJOR (WT.%) AND TRACE ELEMENT (PPM) COMPOSITION OF BASALTIC ROCKS FROM THE SOUTHERN CENTRAL INDIAN RIDGE (GEMINO AREAS EX/FX AND JX)

Stat.	Area	n	SiO_2	Al_2O_3	Fe_2O_3	MnO	MgO	CaO	Na_2O	K_2O	TiO_2	P_2O_5	Cr_2O_3	V_2O_5	Total
25	EX	6	49.87	16.66	9.32	0.16	8.64	12.27	1.91	0.09	1.05	0.03	0.06	0.05	100.11
26	EX	6	50.49	16.32	9.58	0.17	8.23	12.22	1.96	0.12	1.16	0.04	0.05	0.05	100.39
27	FX	6	50.18	17.18	9.25	0.16	7.35	12.47	2.20	0.13	1.16	0.04	0.05	0.05	100.22
38	EX	6	50.68	15.94	9.44	0.17	8.22	12.31	2.23	0.14	1.16	0.05	0.06	0.05	100.45
39	EX	6	50.51	16.31	9.31	0.16	8.72	12.43	1.89	0.08	1.10	0.03	0.06	0.05	100.65
46	EX	1	50.56	15.55	10.11	0.17	8.38	11.85	2.50	0.10	1.28	0.08	0.05	0.05	100.68
53	EX	1	51.09	15.29	10.65	0.19	7.94	11.60	2.48	0.08	1.40	0.09	0.04	0.05	100.86
65	JX	6	50.46	15.48	10.34	0.18	7.64	11.51	2.61	0.24	1.45	0.08	0.04	0.05	100.08
66	JX	6	50.31	15.87	9.48	0.17	8.57	11.58	2.36	0.34	1.25	0.08	0.06	0.04	100.10
69	EX	1	50.52	17.46	8.13	0.14	7.70	13.43	1.95	0.10	0.84	0.04	0.06	0.04	100.45
72	EX	1	50.47	16.97	9.50	0.16	7.88	12.28	2.60	0.10	1.18	0.07	0.05	0.05	101.32
74	EX	3	50.55	17.06	9.04	0.15	8.30	12.57	2.43	0.09	0.66	0.05	0.06	0.04	101.00
75	EX	2	50.92	16.07	9.97	0.16	8.07	12.28	2.38	0.10	1.24	0.06	0.05	0.05	101.35
78	EX	1	50.93	15.75	9.25	0.16	8.15	12.55	2.24	0.09	1.07	0.08	0.06	0.05	100.38
81	EX	6	50.65	15.42	10.74	0.19	7.81	11.71	2.04	0.10	1.42	0.06	0.04	0.05	100.23
82	EX	6	50.85	15.65	10.66	0.19	7.50	11.65	2.20	0.12	1.42	0.06	0.04	0.05	100.33
83	EX	3	48.50	17.80	8.75	0.15	9.96	12.18	1.83	0.06	0.82	0.03	0.05	0.03	100.16

Stat.	Area	n	Nb	Zr	Y	Sr	Co	Ni	Cu	Zn	Ga	FeO_t/MgO
25	EX	6	3	78	24	96	41	153	68	68	16	0.97
26	EX	6	4	86	26	95	40	136	72	72	16	1.05
27	FX	6	4	86	26	103	39	107	69	69	16	1.13
38	EX	6	4	87	25	108	404	110	70	70	15	1.03
39	EX	6	4	80	25	95	42	141	69	69	16	0.96
46	EX	1	n.d.	91	29	104	41	134	69	74	18	1.09
53	EX	1	n.d.	93	32	97	39	112	66	80	17	1.21
65	JX	6	7	119	31	135	42	98	77	77	17	1.21
66	JX	6	9	103	26	142	41	159	71	71	16	1.00
69	EX	1	n.d.	53	20	82	32	104	100	59	16	0.95
72	EX	1	n.d.	81	26	104	34	120	70	66	17	1.08
74	EX	3	n.d.	65	21	93	37	131	63	63	15	0.98
75	EX	2	n.d.	84	28	101	36	113	73	73	17	1.11
78	EX	1	n.d.	73	25	102	37	99	75	65	14	1.02
81	EX	6	4	103	32	96	43	113	82	82	17	1.24
82	EX	6	4	105	32	105	42	108	80	80	17	1.27
83	EX	3	3	60	18	98	44	222	59	59	14	0.79

Total Fe expresssed as Fe_2O_3

Basalt alteration

Talus blocks at fault scraps and slopes of volcanic cones in areas EX/FX and JX commonly have 1–3 mm-thick coatings of Mn oxyhydroxides, mainly todorokite. White, clay-like alteration products on some bleached glass crusts from the top of the central ridge in area JX and the southern propagator in area EX/FX were identified as a mixture of smectite and Ca-zeolites, such as stellerite, gismondite, and mordenite. These minerals suggest hydrothermal alteration different from normal seafloor weathering (Honnorez 1981). Haymon & Kastner (1986) have shown that smectites on hydrothermally altered basalts of the EPR were formed at temperatures as high as 290°C and 360°C, but considerably lower temperatures (less than ~50° C) of smectite formation are also reported (Alt & Honnorez 1984). The formation temperature of smectites and zeolites found in areas EX/FX and JX is not known.

Sediment composition

Sediment samples were obtained off-axis in areas

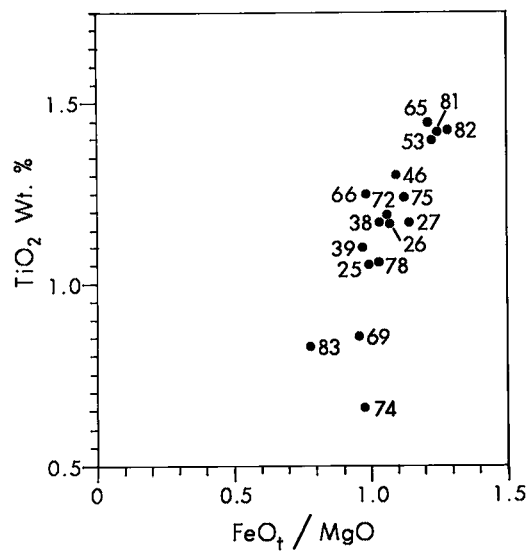

FIG. 6. FeO_t/MgO *versus* TiO_2 diagram for basalts from areas EX/FX and JX. A sample from the axial plateau in area JX (65) is the most fractionated.

TABLE 2. AVERAGE MAJOR AND TRACE ELEMENT COMPOSITION OF HYDROTHERMALLY INFLUENCED SEDIMENTS FROM AREA EX/FX, AND DETRITAL-RICH SEDIMENTS FROM THE CARLSBERG AND EQUATORIAL CENTRAL INDIAN RIDGE (6°N-5.5°S). DATA ARE GIVEN ON A CARBONATE-FREE BASIS

	EX/FX			6°N - 5.5°S		
	n	x	s	n	x	s
wt.%						
Fe_2O_3	85	10.43	3.67	111	7.96	13.86
MnO	85	1.17	0.43	111	0.65	1.90
TiO_2	85	0.35	0.15	111	0.74	1.07
K_2O	85	1.22	0.39	111	2.62	5.19
P_2O_5	85	0.62	0.19	111	0.44	1.22
SiO_2	85	19.60	7.67	111	62.26	22.11
Al_2O_3	85	4.81	2.11	111	11.92	19.08
MgO	85	4.51	1.85	111	8.32	17.43
$CaCO_3$	85	86.00	5.00	111	66.00	19.00
ppm						
Pb	80	69	52	96	30	70
Ba	80	2233	616	96	4733	15832
As	36	197	77	96	126	311
Zr	80	152	39	96	195	387
Y	80	138	42	96	112	311
Rb	80	59	19	96	92	161
Ga	46	5	5	96	19	40
Zn	80	204	59	96	231	507
Cu	80	330	104	96	445	1646
Ni	76	74	54	96	219	334
Co	80	75	48	96	68	158

EX/FX and JX by gravity coring and, where possible, by box corer closer to the rift axis. These were analyzed for major- and trace-element compositions in a search for hydrothermal signatures.

The sediments are brownish yellow and consist mainly of calcareous ooze averaging 85% $CaCO_3$. Feldspar, quartz, and traces of kaolinite, chlorite and illite were detected in the carbonate-free fraction. In some cores, volcanic glass, Fe oxyhydroxides, and Mn micronodules occur. Sediments from area EX/FX are characterized by higher concentrations of Fe_2O_3 and MnO, and lower concentrations of K_2O, Al_2O_3 and SiO_2 than sediments from the CR and the equatorial CIR sampled during GEMINO – 1 (Table 2). The Fe_2O_3 content on a carbonate-free basis averages >10%. The data refer to average core values; metal enrichment was not found in the surface layer. The composition of sediments from area JX corresponds to those of area EX/FX. For comparison, sediment core samples in the TAG hydrothermal field, Mid-Atlantic Ridge, average about 17% Fe_2O_3, and surface samples contain up to 25% Fe_2O_3 (Shearme *et al.* 1983).

Normative sediment analyses have been done using the models of Bischoff *et al.* (1979) and Dymond (1981), which attempt to quantify the composition according to various end-member sediment types. Both models indicate a significant hydrothermal component averaging 40% in the sediments from areas EX/FX and JX. In contrast, equatorial sediments contain ≤10% of a hydrothermal component (Scholten 1987).

In a Fe–Mn–Al ternary diagram (Fig. 7), sediments from area EX/FX plot in the vicinity of "Green Galapagos Clay" (GGC) and "East Pacific Rise Deposits" (EPRD) of Boström *et al.* (1976). The same trend is observed in a Zn–Ni–Cu plot (Fig. 7). By contrast, sediments from the CR (6°N) plot close to the reference sample for terrigenous matter. However, ternary plots are based on relative proportions only; the absolute concentrations of Cu and Zn in the RTJ samples are much lower than those of the EPR sediments.

Heat flow

Heat-flow values obtained in area EX/FX range between 2.4 and 4.4 heat-flow units (HFU) (Table 3). Three measurements taken 10, 19 and 31 km from the ridge axis give an average of 3.4 HFU, which is considerably higher than the average value of 1.5 HFU determined for the CR (Plüger 1985), and 1.4 HFU for the CIR (Langseth & von Herzen 1970). Although the data from area EX/FX are limited, the crustal heat, and hence the conductive heat transport, in segment SCIR I appears to be slightly higher than farther north at the CIR and CR. However, conductive heat flow measured in area EX/FX is within the background values of 2.0–8.6 HFU determined in the TAG hydrothermal field (Rona *et al.* 1984).

Water geochemistry

Area EX/FX. Water samples were taken at 24 locations (Fig. 3a) and analyzed for their total dissolvable Mn (TDM) concentrations. CH_4 values were determined in water samples from 13 stations, and δ^3He in 8 samples from 2 stations. A NW–SE topographic section showing TDM concentrations is given in Figure 8. Although anomalous Mn values are irregularly distributed, the highest values are within 100 m above bottom. The distribution pattern appears to outline a hydrothermal plume which may result from one or more discharge sites.

A maximum value of 27.5 nmol/kg TDM was detected 10 m above bottom (3414 m) at station 74 in the rift valley of the northern propagator. This maximum contrasts with a background value of <1.5 nmol/kg TDM. CH_4 anomalies up to 45.6 nL/L CH_4 above the background of 10 nL/L CH_4 also occur in area EX/FX (*e.g.*, station 01, Fig. 9). These CH_4 anomalies are not reflected by TDM values; however, a potential temperature anomaly of +0.01°C was noted at station 01. Although station 01 has two anomalies below about 150 m, station 79 lacks significant anomalies, and station 35 has a CH_4 enrichment about 220 m

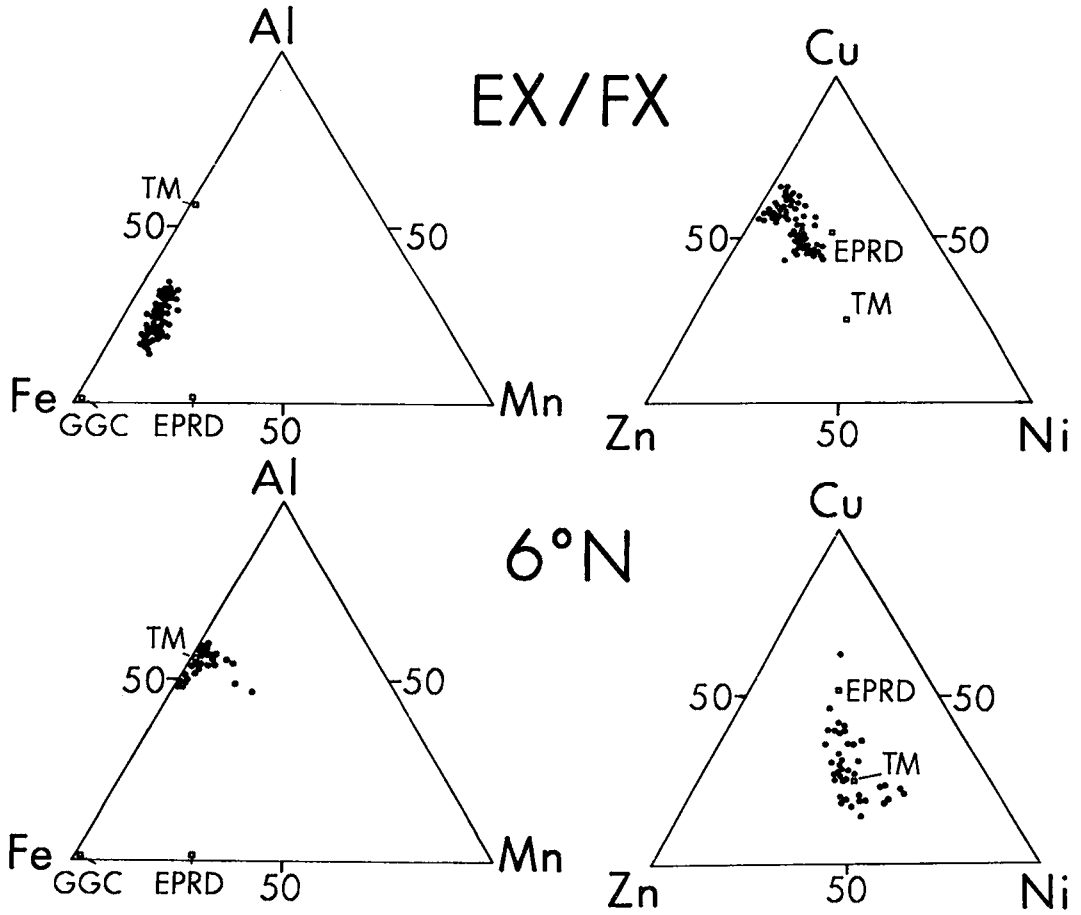

FIG. 7. Fe–Mn–Al and Zn–Ni–Cu ternary diagrams showing that sediments from area EX/FX are closer in composition to "Green Galapagos Clay" (GGC) and "East Pacific Rise Deposit" (EPRD) than sediments from 6°N (CR), which plot close to "Terrigeneous Matter" (TM). Analyses of GGC, EPRD and TM are from Boström *et al.* (1976).

above bottom at 3456 m (Fig. 9). Thus, the data are insufficient to define a plume.

South of the overlap zone in area EX/FX, a series of CH_4 anomalies was found between 21°28′–21°30′S, north of the southern topographic high, and farther south (Fig. 10). Stations 03 and 29 show at least two distinct maxima, which may reflect an irregular hydrothermal plume. A potential temperature anomaly of +0.01°C is associated with a significant CH_4 and a smaller Mn anomaly, occurring 100 m above bottom at station 03.

The distribution of $^3He/^4He$ ratios in the water column in area EX/FX was obtained from stations 55 and 63, respectively north and south of the overlapping spreading center (Table 4). Two samples at 475 m and 775 m above bottom at station 55 revealed δ^3He values of ~18.5%. The δ^3He depth profile at station 63, north of the topographic high at 21°31′S, shows maxima of ~18% δ^3He between 70 m and 1070 m above bottom (Fig. 11). According to data from the equatorial CIR (Plüger 1985), the background was defined to be 10–13% δ^3He. However, this is much less than reported from the EPR 21°N, where background values range up to 30–33% δ^3He and anomalies to 47% δ^3He, respectively (Lupton *et al.* 1980).

Area JX. In area JX, water samples were collected at 9 locations (Fig. 5a) and analyzed for TDM. Samples of 4 stations were analyzed for CH_4. CH_4 anomalies were found at stations 49 and 09 on the northern edge of the central ridge. At station 49 only the top sample at 410 m above bottom showed an enrichment to 27.6 nL/L CH_4; at station 09, all samples are anomalous with the highest value at 410 m (Fig. 12). Significant Mn anomalies up to 10.7 nmol/kg were detected at station 53, at the eastern flank of the central ridge, close to the CH_4 anomalous locations, and at station 58 at the eastern wall of the rift valley, close to the transform fault. A significant potential temperature anomaly of

TABLE 3. CONDUCTIVE HEAT FLOW DATA FOR AREA EX/FX

Station	Distance from ridge axis (km)	Conductivity W/Ksec	Heat Flow mW/msec	HFU
49	10 E	0.966	137.4	3.3
58	19 W	-	184.9	4.4
62	31 E	0.958	100.6	2.4

+0.04°C was found on top of the eastern flank of the central ridge close to station 53.

Discussion

Area EX/FX. Area EX/FX is in the central part of segment SCIR I (strike length of 190 km), about 80 km south of the northern transform fault (Fisher *et al.* 1971), and 70 km north of the southern transform fault. This area is of considerable interest for testing the Francheteau & Ballard (1983) model for a ridge segment spreading at an intermediate rate. According to this model, topographic highs midway between transform faults represent loci of magma upwelling and hydrothermal activity, characterized by an increase in the ratio of sheet flows to pillow lavas, and a decrease in abundance of tectonic fissures. High-level magma chambers were found to be associated with a lower degree of fractionation, which increases systematically away from the topographic high (Thompson *et al.* 1985).

The most significant structural features of area EX/FX are: (i) two overlapping propagators enclosing a 200-m-relief topographic high, and (ii) an axial topographic high towards the south of the mapped area. The overlap zone consists of moderately sedimented sheet flows and appears to be an old and passive feature. It may be compared to Endeavor "Seamount", between West and Middle Valley at the Juan de Fuca Ridge, which was found to be old oceanic crust with no hydrothermal activity (S.D. Scott, pers. comm. 1987). At the southern topographic high, slightly sedimented glassy sheet flows predominate over pillow lavas. Although there is a variability in basalt composition, a systematic variation towards this high was not found. The observed compositional range might be due to magma mixing or small-scale mantle heterogeneities which complicate the simple fractionation pattern.

However, some basalts from the southern propagator close to the topographic high are altered differently from that expected by seafloor weathering, *i.e.*, they have bleached glass crusts which are covered by smectite and Ca-zeolites. This type of alteration was never found in dredge hauls from the CR and equatorial CIR, or in areas other than EX/FX and JX sampled between 21° and 23°S. Although the formation temperature is not known, this alteration assemblage is supposed to be of hydrothermal origin rather than due to seawater–basalt interaction at ambient temperatures (*cf.* Honnorez 1981).

The composition of the sediments from area EX/FX consistently indicates a contribution from

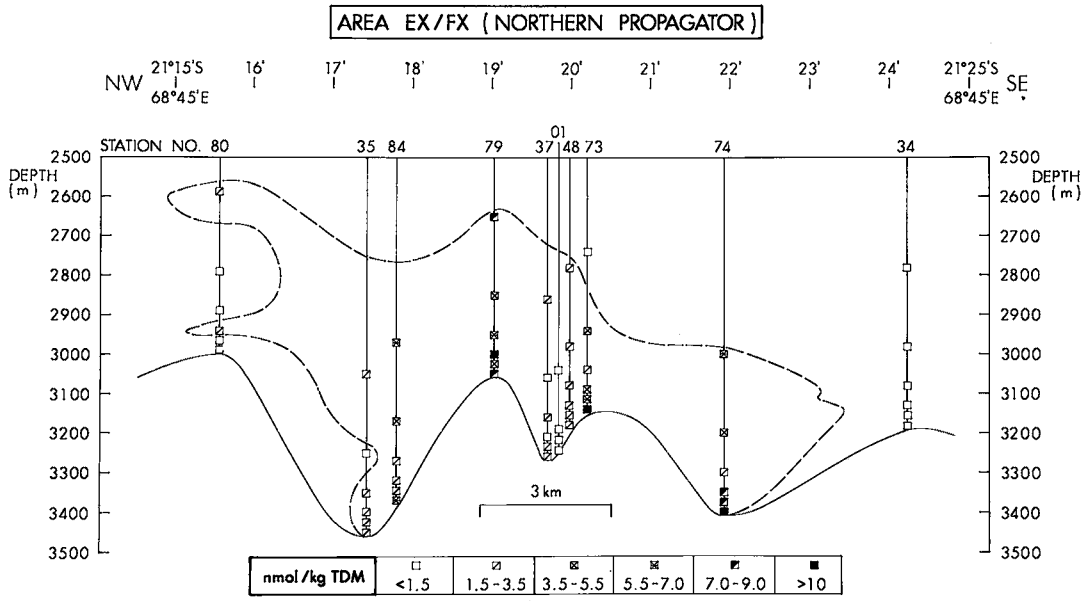

FIG. 8. NW–SE projected section in northern area EX/FX, showing total dissolvable manganese (TDM) in lower water column, and simplified bottom topography. The dashed line outlines all TDM values ≥1.5 nmol/kg, except at stations 37 and 01.

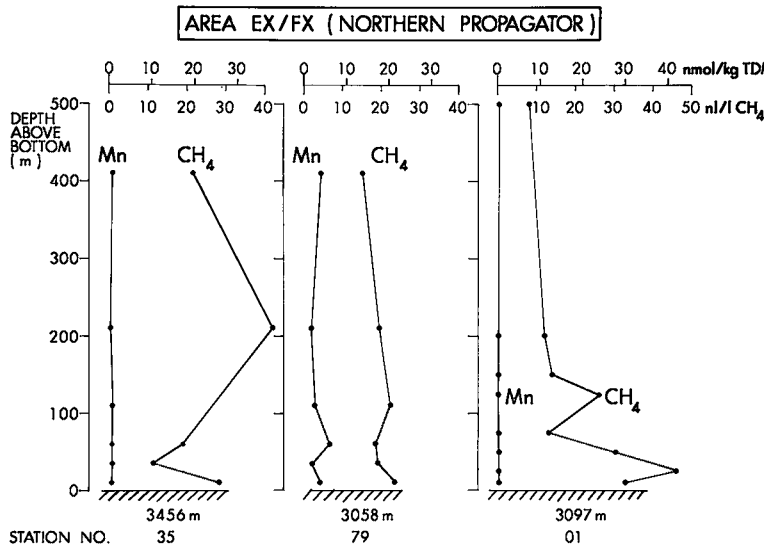

FIG. 9. Total dissolvable manganese (TDM) and CH_4 concentrations in water samples from stations 35, 79 and 01 in the northern part of area EX/FX.

a hydrothermal source and coincides with data by Boström & Fisher (1971), who reported an Fe enrichment in sediments sampled between 22° and 28°S. However, as the hydrothermal input is relatively low compared to sediments from the EPR (Boström *et al.* 1976) and the TAG hydrothermal field (Shearme *et al.* 1983), there must not have been intensive hydrothermal discharge at area EX/FX.

Water geochemistry also yields evidence for low-intensity hydrothermal venting in, or close to, area EX/FX. A single anomaly of 27.5 nmol/kg TDM (station 74) and several smaller anomalies (5–10 nmol/kg TDM) in the rift valley of the northern propagator are comparable with the concentration of dissolved Mn given by Klinkhammer *et al.* (1986) for the vicinity of the TAG area. CH_4 anomalies up to 45.6 nL/L detected at station 01 are also in the range of anomalies found in the TAG area, where CH_4 concentrations >25 nL/L CH_4 outline a hydrothermal plume with a maximum of 105 nL/L CH_4 at a background of 8 nL/L CH_4 (Charlou *et al.* 1987). TDM and CH_4 anomalies in the northern propagator of area EX/FX are not coincident, although potential temperature and δ^3He anomalies provide local evidence for a hydrothermal source in the area. In the southern propagator, the distribution of CH_4 in the water column is also anomalous. It matches up with anomalies in TDM, potential temperature and δ^3He just north of the southern topographic high, where altered basalts occur. The δ^3He values are within background for the TAG area (Rona *et al.* 1984) and indicate a less intense hydrothermal discharge.

The interpretation of water anomalies is likely to be complicated by the effects of bottom currents, such as the Antarctic Bottom Water. Kolla *et al.* (1976) reported for the RTJ area moderate to strong bottom currents in a northeasterly direction. This is also obvious from seafloor photographs which show ripplemarks on the sediment. Thus, the irregular distribution of the Mn and CH_4 anomalies may be explained by the interdigitation of composite plumes which were merged by bottom currents. These currents might even have prevented colloidal hydrothermal material from settling onto coarser pelagic sediment.

Area JX. Area JX includes two-thirds ridge segment SCIR III (strike length 40 km) and the northern fracture zone. According to the model of Francheteau & Ballard (1983), proximity to fracture zones, which mark the cooling edges of a magma chamber, is not favorable for sites of hydrothermal activity. However, area JX may represent a small-scale analog to the MARK (Mid-Atlantic Ridge at the Kane fracture zone, 23°N) area, where the Snakepit hydrothermal field was found at the crest of a central neovolcanic ridge, about 30 km south of the ridge-transform intersection (Karson *et al.* 1987, ODP Leg 106 Scientific Party 1986). In fact, elevated CH_4 and TDM values, and a potential temperature anomaly of 0.04°C were detected in the water column overlying the central ridge in area JX. Here, too, basalts show indications of hydrothermal alteration of the type found in area EX/FX. Aphyric sheet flows from the 3400-m plateau just south of the central ridge are enriched in incompatible elements such as K, Sr, Zr and Nb. Recent studies of basalts from Southern Explorer Ridge, NE Pacific,

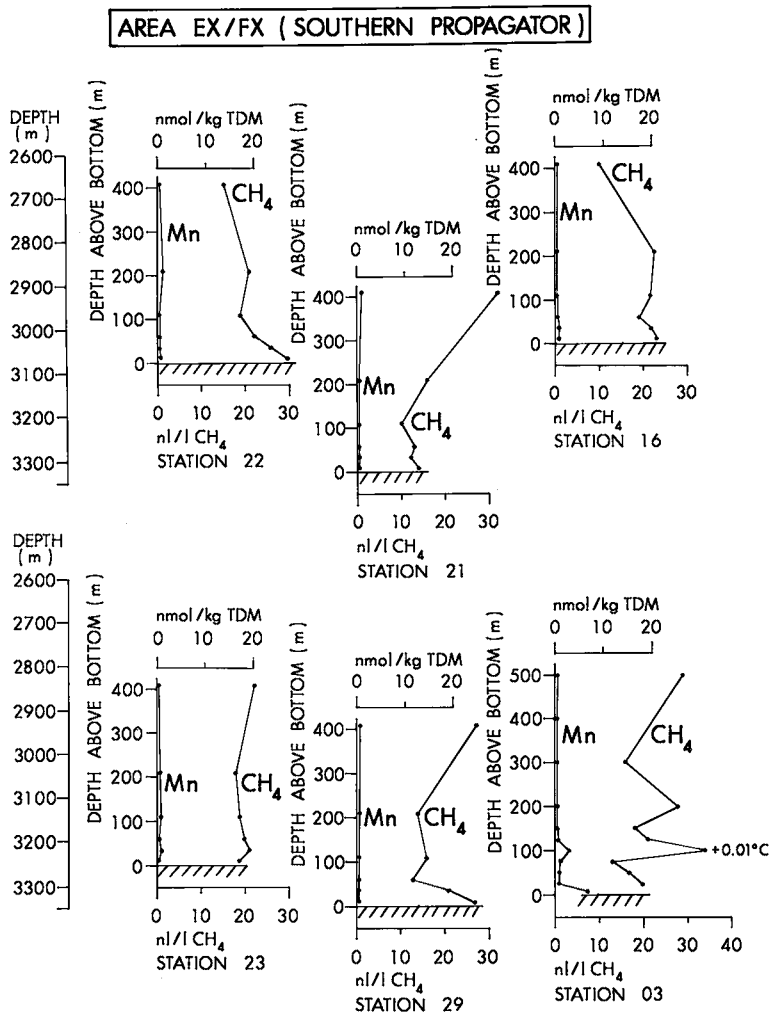

FIG. 10. Total dissolvable manganese (TDM) and CH_4 concentrations in water samples from stations 22, 21, 16, 23, 29 and 03, in the southern part of area EX/FX. Note potential temperature anomaly associated with CH_4 maximum at station 03.

TABLE 4. δ^3He (%)* IN WATER SAMPLES FROM THE NORTHERN (55) AND SOUTHERN (63) AREA EX/FX

Station	Depth (m)	δ^3He (%)
55	2715	18.50 + 0.14
	3015	18.42 + 0.12
63	1215	9.03 + 0.08
	2215	17.56 + 0.26
	2515	18.64 + 0.08
	2815	17.27 + 0.26
	3215	18.06 + 0.08

*δ^3He (%) = 100 (R_{sample}/R_{air}-1) where R = ^{3}He/^{4}He

suggest that enrichment in incompatible (LIL) elements is highest in crestal areas near hydrothermal deposits (Scott *et al.* in prep.). The sediments in area JX reveal a hydrothermal input almost identical to that in area EX/FX and average >10% Fe_2O_3. An irregular, chimney-like structure of unknown composition, but seemingly not basalt, was photographed at the top of a fault scarp at the eastern flank of the central ridge (Fig. 13). As red oxidation colors are not seen in color photographs, sulfides can be ruled out. However, this structure could consist of low-temperature hydrothermal products such as amorphous silica, as recently described from the Galapagos Spreading Center at 86°W (Herzig *et al.* 1988).

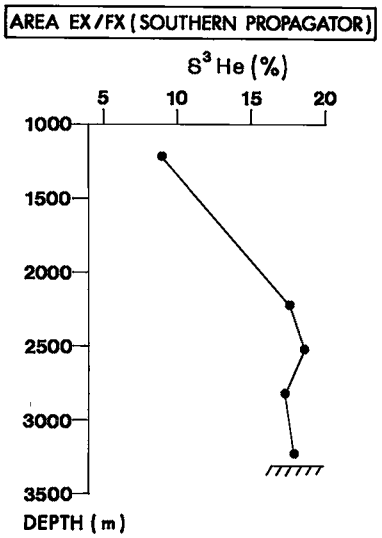

FIG. 11. δ^3He depth profile for station 63 in the southern part of area EX/FX.

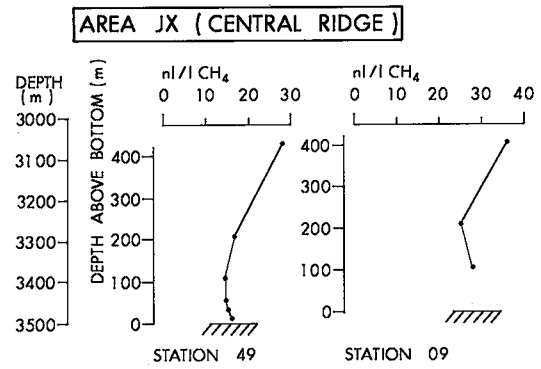

FIG. 12. CH_4 concentrations in water samples from stations 49 and 09 at the northern edge of the central ridge in area JX.

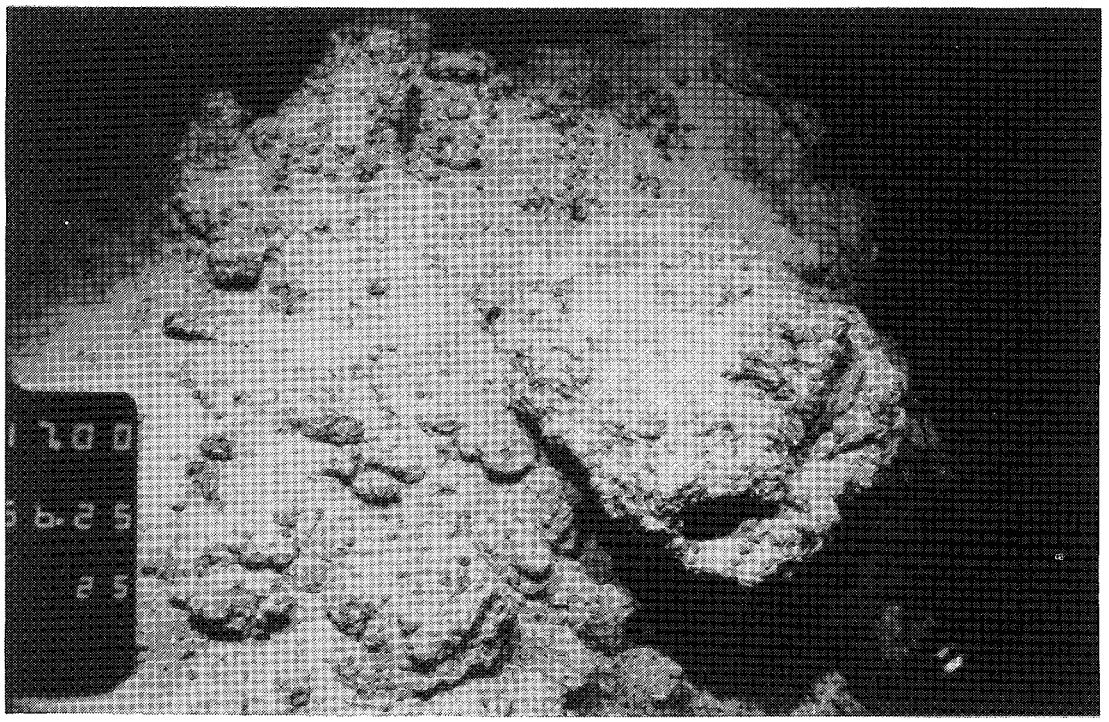

FIG. 13. Seafloor photograph showing irregular chimney-like structure of possible hydrothermal origin at the top of a fault scarp at the eastern flank of the central ridge in area JX (69°09.8′E, 22°55.3′S, 3340-m water depth). The long side of the photograph is about 3.5 m.

SUMMARY AND CONCLUSIONS

In the present study, the CIR at about 21.5°S (area EX/FX) and 23°S (area JX) has been mapped, photographed, and sampled in an attempt to locate sites of fossil or recent hydrothermal activity. Hydrocast

and sediment anomalies occur in the northern and southern propagator of the overlapping spreading center in area EX/FX. These anomalies probably originate from more than one low-temperature vent site. A distinct CH_4, TDM and δ^3He anomaly, altered basalts, and increase in potential temperature were found just north of the southern topographic high in area EX/FX. Thus, this structure might be associated with hydrothermal venting. The central neovolcanic ridge appears to be the focus of hydrothermal activity in area JX. This is indicated by hydrocast data, a potential temperature anomaly, and basalt alteration. In comparison to data reported from the TAG hydrothermal field at the Mid-Atlantic Ridge, which is the only known site of high-temperature hydrothermal discharge at a slow-spreading oceanic ridge, the results obtained from the present study so far suggest only a weak and probably lower temperature hydrothermal activity. However, both locations, the southern topographic high in area EX/FX, and the central ridge in area JX, require further investigation.

Acknowledgements

The authors acknowledge funding of the GEMINO project by a grant from the Bundesminister für Forschung und Technologie, Bonn (FRG) to G.H. Friedrich (Technische Hochschule Aachen). We are particularly grateful to R. Schlich (Institut de Physique du Globe de Strasbourg), J. Francheteau and P. Patriat (Institut de Physique du Globe de Paris) for providing unpublished magnetic and bathymetrical data. Captains, officers and crew of *RV SONNE*, as well as Preussag personnel, are thanked for their efforts during our cruises. Thanks are due to W. Roether (Universität Heidelberg) for helium analyses. The manuscript benefitted from comments by S.D. Scott, T.F. McConachy, J.M. Peter, M.C.C. Alton (University of Toronto) and A. Lange (Preussag AG). Thanks are due to the editors of the Special Volume, especially to T.J. Barrett, for many helpful and constructive comments. Reviews by W. Schwab, D. Olson, and an anonymous reviewer considerably improved the manuscript. P.M.H. acknowledges financial support during the writing of this paper from a research fellowship of the Alexander von Humboldt Foundation and a strategic grant of the Natural Sciences and Engineering Research Council of Canada to S.D. Scott and R.L. Chase.

References

Alt, J.C. & Honnorez, J. (1984): Alteration of the upper oceanic crust, DSDP site 417: mineralogy and chemistry. *Contrib. Mineral. Petrology* **82**, 149-169.

Bäcker, H. (1975): Cruise Report VA-07. *Arbeitsgemeinschaft Marine Rohstoffe*. Hannover, FRG.

Bischoff, J.L., Heath, G.R. & Leinen, M. (1979): Nature and origin of metalliferous sediments in DOMES site C, Pacific Manganese Nodule Province. *In* Marine Geology and Oceanography of the Pacific Manganese Nodule Province (J.L. Bischoff & D.Z. Piper, eds.). Plenum Press, New York, 397-436.

Boström, K. & Fisher, D.E. (1971): Volcanogenic uranium, vanadium and iron in Indian Ocean sediments. *Earth Planet. Sci. Lett.* **11**, 95-98.

_____, Joensuu, U., Valdes, S., Charm, W. & Glaccum, R. (1976): Geochemistry and origin of the East Pacific Rise sediments sampled during DSDP Leg 34. *Initial Reports of the Deep Sea Drilling Project* **34**, 559-574. U.S. Goy. Printing Office, Washington, D.C.

Charlou, J.L., Rona, P. & Bougault, H. (1987): Methane anomalies over TAG hydrothermal field on Mid Atlantic Ridge. *J. Mar. Res.* **45**, 461-472.

Corliss, J.B., Dymond, J., Gordon, L.I., Edmond, J.M., von Herzen, R.P., Ballard, R.D., Green, K., Williams, D., Bainbridge, A., Crane, K. & van Andel, T.H. (1979): Submarine thermal springs on the Galapagos Rift. *Science* **203**, 1073-1083.

Dymond, J. (1981): Geochemistry of Nazca plate surface sediments: An evaluation of hydrothermal, biogenic, detrital, and hydrogenous sources. *Geol. Soc. Amer. Mem.* **154**, 133-173.

Fisher, R.L., Sclater, J.G. & McKenzie, D.P. (1971): Evolution of the Central Indian Ridge, Western Indian Ocean. *Geol. Soc. Amer. Bull.* **82**, 553-562.

Francheteau, J., Needham, H.D., Choukroune, P., Juteau, T., Seguret, M., Ballard, R.D., Fox, J.P., Normark, W., Carranza, A., Cordoba, D., Guerrero, J., Rangin, C., Bougault, H., Cambon, P. & Hékinian, R. (1979): Massive deep-sea sulfide ore deposits discovered on the East Pacific Rise. *Nature* **277**, 523-528.

_____ & Ballard, R.D. (1983): The East Pacific Rise near 21°N, 13°N and 20°N: inferences for along-strike variability of axial processes of the Mid-Ocean Ridge. *Earth Planet. Sci. Lett.* **64**, 93-113.

Grobenski, Z., Lehmann, R., Radzink, B. & Voellkopf, U. (1984): Determination of trace metals in seawater using Zeeman graphite furnace AAS. *Atom. Spec.* **5**, 87-90.

Haymon, R.M. & Kastner, M. (1986): The formation of high temperature clay minerals from basalt alteration during hydrothermal discharge on the East Pacific Rise axis at 21°N. *Geochim. Cosmochim. Acta* **50**, 1933-1939.

HÉKINIAN, R. (1982): *Petrology of the Ocean Floor.* Elsevier, Amsterdam.

———, FEVRIER, M., NEEDHAM, H.D., AVEDIK, F. & CAMBON, P. (1981): Sulfide deposits, East Pacific Rise near 13°N. *EOS, Trans. Amer. Geophys. Union* **62**, 913.

HERZIG, P.M., BECKER, K.P., STOFFERS, P., BÄCKER, H. & BLUM, N. (1988): Hydrothermal silica chimney fields at the Galapagos Spreading Center at 86°W. *Earth Planet. Sci. Lett.* **89**, 261-272.

HONNOREZ, J. (1981): The aging of the oceanic crust at low temperature. *In* The Sea 7, The Oceanic Lithosphere (C. Emiliani, ed.). John Wiley & Sons, New York, 525-587.

JENKINS, W.J., COLLENTRO, W.V. & BOUDREAU, R.D. (1979): W.H.O.I. Helium Isotope Laboratory Data Release No. 1. *Woods Hole Oceanographic Institution,* Woods Hole, Mass.

KARSON, J.A., THOMPSON, G., HUMPHRIS, S.E., EDMOND, J.M., BRYAN, W.B., BROWN, J.R., WINTERS, A.T., POCKALNY, R.A., CASEY, J.F., CAMPBELL, A.C., KLINKHAMMER, G., PALMER, M.R., KINZLER, R.J. & SULANOWSKA, M.M. (1987): Along-axis variations in seafloor spreading in the MARK area. *Nature* **328**, 681-685.

KLINKHAMMER, G., ELDERFIELD, H., GREAVES, M., RONA, P. & NELSEN, T. (1986): Manganese geochemistry near high-temperature vents in the Mid-Atlantic Ridge valley. *Earth Planet. Sci. Lett.* **80**, 230-240.

KOLLA, V., SULLIVAN, L., STREETER, S.S. & LANGSETH, M.G. (1976): Spreading of Antarctic bottom water and its effects on the floor of the Indian Ocean inferred from bottom-water potential temperature, turbidity, and sea-floor photography. *Mar. Geol.* **21**, 171-189.

KOSKI, R.A., GOODFELLOW, R. & BOUSE, R.M. (1982): Preliminary description of massive sulfide samples from the southern Juan de Fuca Ridge. *U.S. Geol. Surv. Open-File Rep.* **82-200B**.

LANGSETH, M.G. & VON HERZEN, R.P. (1970): Heat flow through the floor of the world oceans. *In* The Sea 4 (A.E. Maxwell, ed.). Interscience, New York, 299-352.

LONSDALE, P.F., BISCHOFF, J.L., BURNS, U.M., KASTNER, M. & SWEENEY, R.E. (1980): A high-temperature hydrothermal deposit on the sea bed at a Gulf of California spreading center. *Earth Planet. Sci. Lett.* **49**, 8-20.

LUPTON, J.E., KLINKHAMMER, G.P., NORMARK, W.R., HAYMON, R., MACDONALD, K.C., WEISS, R.F. & CRAIG, H. (1980): Helium-3 and manganese at the 21°N East Pacific Rise hydrothermal site. *Earth Planet. Sci. Lett.* **50**, 115-127.

MACDONALD, K.C. & FOX, P.J. (1983): Overlapping spreading centers: New accreting geometry on the East Pacific Rise. *Nature* **301**, 55-58.

MICHARD, A., MONTIGNY, R. & SCHLICH, R. (1986): Geochemistry of the mantle beneath the Rodriguez Triple Junction and the South-East Indian Ridge. *Earth Planet. Sci. Lett.* **78**, 104-114.

MONTIGNY, R., MICHARD, A. & SCHLICH, R. (1985): Isotope geochemistry of the mantle beneath the Rodriguez Triple Junction (Indian Ocean). *Terra Cognita* **5**, 181-182 (abstr.).

NORMARK, W.R., LUPTON, J.E., MURRAY, J.W., KOSKI, R.A., CLAGUE, D.A., MORTON, J.L., DELANEY, J.R. & JOHNSON, H.P. (1982): Polymetallic sulfide deposits and water column tracers of active hydrothermal vents on the southern Juan de Fuca Ridge. *Mar. Tech. Soc. J.* **16**, 46-53.

ODP LEG 106 SCIENTIFIC PARTY (1986): Drilling the Snakepit hydrothermal sulfide deposit on the Mid-Atlantic Ridge, Lat. 23°22'N. *Geology* **14**, 1004-1007.

PLÜGER, W.L. (1985): Fahrtbericht SO-28 und Wissenschaftlicher Bericht GEMINO-1: Geothermal Metallogenesis Indian Ocean. BMFT 03 R 339, *Institut für Mineralogie und Lagerstättenlehre,* RWTH Aachen, FRG.

——— & HERZIG, P.M. (1986): Geothermal metallogenesis Indian Ocean – results of recent exploration in the Rodriguez Triple Junction area. *Int. South. Europ. Symp. Expl. Geochem., Athens, IGME-AEG,* 60 (abstr.).

———, FRIEDRICH, G., HERZIG, P.M., KUNZENDORF, H., STOFFERS, P., WALTER, P., SCHOLTEN, J., MICHAELIS, W. & MYCKE, B. (1984): Prospektion hydrothermaler Mineralisationen am Mittelozeanischen Rücken des Indischen Ozeans. *Bundesministerium für Forschung und Technologie, Status Bericht,* PLR-KFA Jülich, FRG, 471-488.

PRICE, R.C., KENNEDY, A.K., RIGGS-SNEERINGER, M. & FREY, F.A. (1986): Geochemistry of basalts from the Indian Ocean triple junction: implications for generation and evolution of Indian Ocean ridge basalts. *Earth Planet. Sci. Lett.* **78**, 379-396.

ROETHER, W. (1983): Tracing water flow in the ocean. *Nature* **302**, 380.

RONA, P.A., BOSTRÖM, K., WIDENFALK, L.E.G., MALLETTE, M. & MELSON, W.B. (1981): Preliminary reconnaissance of the Carlsberg Ridge, northwestern Indian Ocean, for hydrothermal mineralization. *EOS, Trans. Amer. Geophys. Union* **62**, 914.

———, THOMPSON, G., MOTTL, M.J., KARSON, J.A., JENKINS, W.J., GRAHAM, D., MALLETTE, M., VON DAMM, K. & EDMOND, J.M. (1984): Hydrothermal activity at the Trans-Atlantic geotraverse hydrothermal field, Mid-Atlantic Ridge crest at 26°N. *J. Geophys. Res.* **89**, 11365-11377.

_____, KLINKHAMMER, G., NELSEN, T.A., TREFRY, J.H. & ELDERFIELD, H. (1986): Black smokers, massive sulphides and vent biota at the Mid-Atlantic Ridge. *Nature* **321**, 33-37.

ROZANOVA, T.V. & BATURIN, G.N. (1971): Hydrothermal ore shows on the floor of the India Ocean. *Oceanology* **11**, 874-879.

SCHLICH, R. (1982): The Indian Ocean: aseismic ridges, spreading centers and ocean basins. *In* The Ocean Basins and Margins **6** (A.E.M. Nairn & F.G. Stehli, eds.). Plenum Press, New York, 51-147.

_____, MUNSCHY, M., ROYER, J.Y., MONTIGNY, R. & WHITECHURCH, H. (1986): Proposal for oceanic drilling at the Rodriguez Triple Junction (Indian Ocean). *Ocean Drilling Program,* Texas A & M University, U.S.A.

SCHOLTEN, J. (1987): *Ein Beitrag zur Geochemie und Sedimentationsgeschichte am Carlsberg-und Mittelindischen Rücken.* Diss. Univ. Heidelberg, FRG.

SCLATER, J.G., FISHER, R.L., PATRIAT, P., TAPSCOTT, C. & PARSONS, B. (1981): Eocene to recent development of the South-west Indian Ridge, a consequence of the evolution of the Indian Ocean Triple Junction. *Geophys. J. Roy. Astron. Soc.* **64**, 587-604.

SCOTT, S.D., BARRETT, T.J., HANNINGTON, M.D., CHASE, R.L., FOUQUET, Y. & JUNIPER, K. (1984): Tectonic framework and sulfide deposits of the Southern Explorer Ridge, Northeastern Pacific Ocean. *EOS, Trans. Amer. Geophys. Union* **65**, 1111.

SHEARME, S., CRONAN, D.S. & RONA, P.A. (1983): Geochemistry of sediments from the TAG hydrothermal field, Mid-Atlantic Ridge at latitude 26°N. *Mar. Geol.* **51**, 269-291.

SPIESS, F.N., MACDONALD, K.C., ATWATER, T., BALLARD, R., CARRANZA, A., CORDOBA, D., COX, C., DIAZ GARCIA, V.M., FRANCHETEAU, J., GUERRERO, J., HAWKINS, J., HAYMON, R., HESSLER, R., JUTEAU, T., KASTNER, M., LARSON, R., LUYENDYK, B., MACDOUGALL, J.D., MILLER, S., NORMARK,W., ORCUTT, J. & RANGIN, C. (1980): East Pacific Rise: hot springs and geophysical experiments. *Science* **207**, 1421-1444.

SWINNERTON, J.W. & LINNENBOM, V.J. (1967): Determination of the C_1 to C_4 hydrocarbons in sea water by gas chromatography. *J. Chromat. Sci.* **5**, 570-573.

TAPSCOTT, G.R., PATRIAT, P., FISHER, R.L., SCLATER, J.G., HOSKINS, H. & PARSONS, B. (1980): The Indian Ocean triple junction. *J. Geophys. Res.* **85**, 4723-4739.

THOMPSON, G., BRYAN, W.B., BALLARD, R., HAMURO, K. & MELSON, W.G. (1985): Axial processes along a segment of the East Pacific Rise, 10°–12°N. *Nature* **318**, 429-433.

VON HERZEN, R.P. & MAXWELL, A.E. (1959): The measurement of thermal conductivity of deep-sea sediments by a needle probe method. *J. Geophys. Res.* **64**, 1557-1563.

Received October 16, 1987; revised manuscript accepted May 13, 1988.